





# Hall anomaly by vacancies in a pinned lattice of vortices: A quantitative analysis based on the thin-film data from $\text{Bi}_{2.1}\text{Sr}_{1.9}\text{CaCu}_{2.0}\text{O}_{8+\delta}$

Ruonan Guo , Yong-Cong Chen ,\* and Ping Ao <sup>†</sup>

Shanghai Center for Quantitative Life Sciences & Physics Department, Shanghai University, Shanghai 200444, China

 (Received 25 April 2022; revised 19 July 2022; accepted 30 August 2022; published 12 September 2022)

The Hall anomaly, as appears in the mixed-state Hall resistivity of type-II superconductors, has been the subject of numerous theories, but there is not yet a consensus on its origin. In this paper, we conduct a quantitative analysis of the magnetotransport measurements on  $\text{Bi}_{2.1}\text{Sr}_{1.9}\text{CaCu}_{2.0}\text{O}_{8+\delta}$  (BSCCO) thin films by Zhao *et al.* [Phys. Rev. Lett. **122**, 247001 (2019)] and validate a previously proposed vacancy mechanism [cf. Ao, J. Phys. Condens. Matter. **10**, L677 (1998)] with many-body vortex correlations for the phenomenon. The model attributes the Hall anomaly to the motion of vacancies in pinned fragments of the vortex lattice. Its validity is first examined by an exploration of the vortex states near the Kosterlitz-Thouless transition on the vortex crystal. Comparisons are then carried out between the measured activation energies with the calculated creation energy of the vortex-antivortex pair and the vacancy energy on the flux-line lattice, with no adjustable parameter. Our analysis elucidates the theoretical basis and prerequisites of the vacancy model. In particular, the vacancy activation energies are an order of magnitude smaller than that of a sole vortex line. The proposed mechanism may provide a macro-theoretical framework for other studies.

DOI: [10.1103/PhysRevB.106.104507](https://doi.org/10.1103/PhysRevB.106.104507)

## I. INTRODUCTION

The Hall anomaly in the mixed-state Hall resistivity of superconductors, i.e., the sign reversal of the Hall resistivity below the superconducting transition temperature and in the presence of flux-line vortices, was discovered as early as early as the 1950s [1,2]. Much attention has since been given to its physical origin. Prior to the discovery, Onsager [3] had established the framework of the vortex theory based on fluid dynamics in 1949. A modern version of his work, the equation for a  $j$ th vortex of unit length in a superconductor, takes the same Langevin equation as a charged particle in the presence of a magnetic field [4],

$$m\ddot{\mathbf{r}}_j = q\left(\frac{n_s}{2}\right)h(\mathbf{v}_{s,t} - \dot{\mathbf{r}}_j) \times \hat{\mathbf{z}} - \eta\dot{\mathbf{r}}_j + \mathbf{F}_p + \mathbf{f}, \quad (1)$$

where the overhead dots stand for time derivatives. The unit length vortex at  $\mathbf{r}_j$  has an effective mass  $m$ , subject to a pinning force  $\mathbf{F}_p$ , a fluctuating force  $\mathbf{f}$ , and viscosity  $\eta$  and moves in a background of a superfluid with total velocity  $\mathbf{v}_{s,t}$  (which includes contributions from all other vortices). For the parameters in Eq. (1),  $q = \pm 1$  indicates the vorticity (under the usual right-hand rules),  $h$  is the Planck constant,  $n_s$  is the superfluid carrier density, and  $\hat{\mathbf{z}}$  is the unit vector in the direction of the magnetic field. The term with the velocity  $\dot{\mathbf{r}}_j$  on the right-hand side is also known as the Magnus force. Note that cgs units are assumed throughout this paper, in line with the majority of work in the literature.

With Eq. (1), two idealized pictures can be drawn. Take, e.g.,  $q = +1$ ; Fig. 1(a) shows that in the absence of the pin-

ning force  $\mathbf{F}_p$  and the frictional force ( $\eta = 0; \mathbf{F}_p = 0$ ), the vortex velocity  $\dot{\mathbf{r}}_j$  matches that of the superfluid in both direction and magnitude. In other words, for an average charge  $e$  in the vortex, the Magnus force (due to the electric field  $\mathbf{E}$  generated by moving vortex), i.e.,  $e\mathbf{E}$ , cancels the Lorentz force  $(e/c)\mathbf{v}_s \times \mathbf{H}$ , leading to the same Hall effect as in a normal metal. One has no reason to expect a sign reversal of the Hall resistance  $R_{xy}$  below the superconducting transition temperature  $T_c$ . Figure 1(b) presents an alternative scenario of an extreme situation: The vortex is firmly trapped by a strong pinning force  $\mathbf{F}_p$  such that there is no Magnus force. Moreover, the pinning force is opposite to the Lorentz force, and there will be no change in sign of the Hall resistance  $R_{xy}$  either. These scenarios raise an apparent paradox between conceptual reasoning and experimental observation.

Several mechanisms [5–15] have been proposed to address the sign anomaly, which we have summarized in Secs. A and B of the Supplemental Material (SM) [16]. Despite the fact that the Hall anomaly has attracted numerous theoretical studies, a lack of advancement in experimental techniques has hindered a consensus on its origin. However, there has been a steady improvement in the situation over the last two decades. In 1996, Zhu *et al.* [17] designed a mechanical experiment to directly measure the total transverse force on moving vortices in a type-II superconductor for the first time, and their result is consistent with the Ao-Thouless theory [11]. In 2001, Zhu and Nyeanchi [18] demonstrated that certain features of the Kosterlitz-Thouless (KT) transition of a vortex lattice are preserved near the superconducting transition temperature. In 2019, Chen and co-workers [19] developed a fabrication process which can produce intrinsic monolayer crystals of  $\text{Bi}_2\text{Sr}_2\text{CaCu}_2\text{O}_{8+\delta}$  (BSCCO). In 2021, Richter *et al.* [20] measured the resistivity, Hall effect, and anisotropic

\*chenyongcong@shu.edu.cn

<sup>†</sup>aoping@sjtu.edu.cn

superconducting coherence lengths in  $\text{HgBa}_2\text{CaCu}_2\text{O}_6$  (HBCCO) thin films with morphological variations. Excellent measurement of Hall effects in an atomically thin high-temperature superconductor by Zhao *et al.* [21] in 2019 drastically extended the region which displays the Hall sign reversal.

In this paper, we present an in-depth analysis of the activation energies deduced from the experimental data in Ref. [21]. It is then compared with the predicted activation energy of independent vortices and the energy of vortex many-body correlation under flux-line lattices. In the next section, we examine whether the abnormal Hall effect on the BSCCO film meets the prerequisites of the vacancy model by analyzing the state of the vortices near the KT transition temperature. In Sec. III, we first review the fundamentals of our methodology, namely, the pinning and dynamics of vacancies in a vortex lattice. The core concept presented follows throughout the entire section. The experimental data are extracted and compared with the theoretical calculations of activation energies of carriers in the BSCCO film, under varying magnetic fields. The excellent agreement between them elucidates the conformation of the Hall anomaly to the vacancy model. Some concluding remarks and possible connections to other works and future directions are discussed in the final section.

## II. VORTEX STATES AROUND THE KOSTERLITZ-THOULESS TRANSITION

To validate that the Hall anomaly complies with the prerequisites of the vacancy model, it is crucial to clarify the states of the vortex crystal near the Kosterlitz-Thouless (KT) transition. In this section, we will first review some basics of the vortex lattice state near the KT transition which melts the crystal. Then we discuss the nature of the KT transition from the thermodynamic perspective and estimate the theoretical value of the transition temperature  $T_{\text{KT}}$  of the BSCCO thin film. Finally, the question of whether the concept and presence of vacancies still apply above  $T_{\text{KT}}$  is addressed.

### A. KT transition of molten crystals

The melting transition of most solid materials at the present has not been well understood as there is a lack of theories explaining the transition on the microscopic scale. Furthermore, the mechanism of melting depends on the interaction details between the constituents forming a crystal lattice. In particular, various defects which reduce the translational order of the crystal play a major role. It should be noted that in two dimensions, only edge dislocations and not the screw ones are important in the melting transition. The core energy of the dislocations upon which these effects can form must be sufficiently low for their spontaneous appearance. The specific analysis of the dislocation formation energy in a two-dimensional (2D) BSCCO film will be presented in the subsequent section.

The dislocations in question are topological point defects, which implies that a single one cannot be created isolated by an affine transformation without cutting the hexagonal crystal up to infinity (i.e., up to its borders). Hence they must be created in pairs with antiparallel Burgers vectors.

If a large number of dislocations were, e.g., thermally excited, the discrete translational order of the crystal would be destroyed. Simultaneously, the shear modulus and Young's modulus would disappear, signaling the starting of the molten transition from a solid to a fluid phase.

However, it is possible that the orientational order is not yet fully destroyed (as indicated by lattice lines in one direction), and one finds—very similar to liquid crystals—a fluid phase with typically a six-folded direction field. This so-called hexatic phase still has an orientational stiffness. Such an anisotropic fluid phase can appear when the dislocations dissociate into isolated five-folded and seven-folded disclinations [22]. This two-step melting phenomenon is described within the so-called Kosterlitz-Thouless-Halperin-Nelson-Young-theory (KTHNY theory), based on two separate transitions of the Kosterlitz-Thouless type. In 2010, Gasser *et al.* [22] presented the first conclusive evidence for the existence of the hexatic phase and two continuous phase transitions in 2D melts in a colloidal model system with repulsive magnetic dipole-dipole interaction.

### B. Thermodynamics of the KT transition

The topological phase transition in a 2D superfluid was predicted by Kosterlitz and Thouless [23] and elaborated by Nelson and Halperin [24] and Nelson [25]. A simple thermodynamic argument allows us to understand the intrinsic quality of the KT transition [26]. The Helmholtz free energy is given by the difference between the energy  $E$  and the entropy of a dislocation  $S$  multiplied by the temperature  $T$ ,

$$F = E - TS. \quad (2)$$

The energy  $E$  is given by Eq. (10), which is contributed by a dislocation pair over a large distance. For convenience, we rewrite it as

$$E = \frac{d\varepsilon_0}{2\sqrt{3}\pi} \ln\left(\frac{L}{a}\right). \quad (3)$$

The entropy can be estimated from the number of places the dislocation can be positioned, namely, on each of the  $\sim L^2$  plaquettes of the lattice, i.e.,

$$S = k_B \ln\left(\frac{L^2}{a^2}\right). \quad (4)$$

Accordingly, the free energy is given by

$$F = \left[ d \frac{\varepsilon_0}{2\sqrt{3}\pi} - 2k_B T \right] \ln\left(\frac{L}{a}\right). \quad (5)$$

Evidently, there exists a temperature above which a vast number of dislocations are preferred. Such a transition is of topological nature and is referred to as the KT transition. The transition temperature  $T_{\text{KT}}$  could be expressed as

$$T_{\text{KT}} = \frac{1}{4\sqrt{3}\pi k_B} \left( \frac{\Phi_0}{4\pi\lambda} \right)^2 d \cong 57.3 \text{ K}. \quad (6)$$

Ideally at  $T < T_{\text{KT}}$ , thermally excited dislocations form close, compact pairs, namely, dislocation pairs. However, they are spontaneously separated when  $T > T_{\text{KT}}$ . The KT transition temperature  $T_{\text{KT}}$  measured by Zhao *et al.* is 60 K [21],

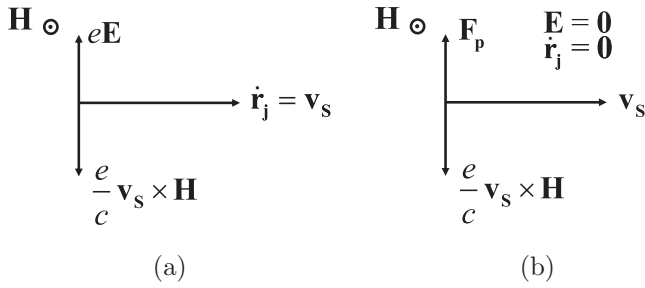


FIG. 1. Analysis of vortex dynamics in two ideal situations. In this figure,  $\mathbf{E}$  is the electric field generated by the moving vortex, and  $\mathbf{H}$  is the applied magnetic field. (a) With no pinning force  $\mathbf{F}_p = 0$  and no frictional force ( $\eta = 0$ ;  $\mathbf{f} = 0$ ), the vortex moves at the same velocity as the superfluid  $\dot{\mathbf{r}}_j = \mathbf{v}_s$ . (b) The vortex is firmly trapped by a strong pinning force  $\mathbf{F}_p$  such that  $\dot{\mathbf{r}}_j = 0$ .

which validates the effective thickness and the London penetration depth chosen below for our analysis.

### C. The presence of vacancies above $T_{KT}$

Let us for the moment assume a vortex solid-liquid phase transition near (the first)  $T_{KT}$ , around 60 K. Then the Arrhenius behavior of longitudinal resistance places the Hall sign reversal within the thermally activated flux flow regime above the vortex lattice melting temperature [27]. An urgent question is whether the Hall anomaly mainly appears in the vortex-liquid regime, scilicet, fades away as the vortex liquid freezes into a solid-state crystal.

However, there is no evidence for such a solid-liquid phase transition in the BSCCO film. As the transition would be a first-order phase transition in which observation of latent heat was to be expected, the resistance of the BSCCO film should measure an abrupt change at the transition. More crucially, the Kosterlitz-Thouless transition is classified as a topological phase transition, the third type of phase transition. Experimentally, all curves intercepted by the isotherm of  $T_{KT} = 60$  K are smooth, with no sign of jump around the node.

According to the generic nature of phase transitions in two-dimensional materials [28–30], we can reasonably deduce the phase diagram as shown in Fig. 2. In the illustration,  $T_{KT}$  is the lowest with a second melting temperature  $T_m$  for the solid-liquid phase transition below the superconducting transition temperature  $T_c$ . For  $T_{KT} < T < T_m$ , there should exist local fragments of vortex lattice, and in each of them, long-range order ought to be preserved. This sets the prerequisites for the existence of vacancies and the applicability of the vacancy model proposed by Ao [4].

## III. HALL ANOMALY BY VACANCIES OF THE VORTEX LATTICE

In this section, we intend to quantitatively demonstrate that the Hall anomaly is in full concert with the theoretical basis of the vacancy hypothesis. Namely, it is due to the movement of vacancies, a direct result of many-body vortex interaction and the origin of the Hall anomaly. First, the dynamics of vacancies in a vortex lattice are discussed in detail. Then some results are applied to fit the experimental data given by Zhao

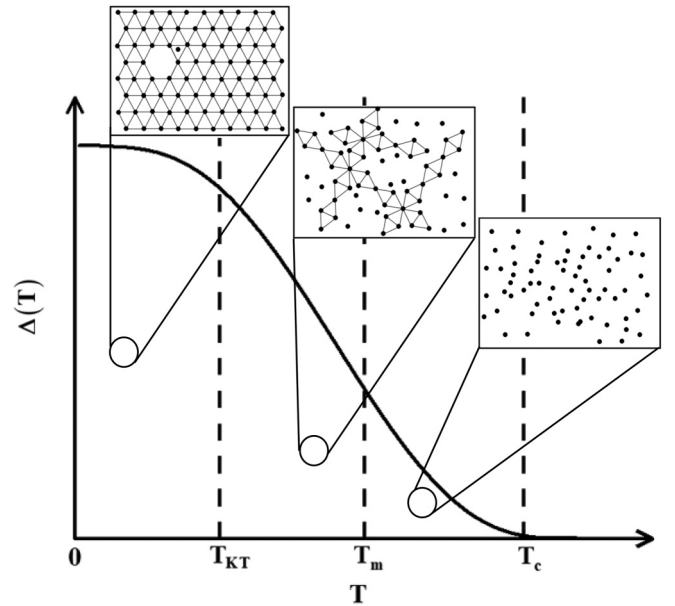


FIG. 2. Schematic phase diagram of the superconducting gap vs temperature. The solid curve represents the relationship between the order parameter and temperature of the type-II superconductor under a constant external magnetic field. When  $T_{KT} < T < T_m$ , the vortex lattice possesses quasi-long-range order. The three insets show the states of the vortex lattice at diverse temperature intervals.

*et al.* [21] with no adjustable parameters. The vacancy activation or formation energy under a diverse set of magnetic fields is found to be of the same order of magnitude as theoretical predictions. In particular, both theoretical and experimental results show that the energy of an independent vortex line or a vortex-antivortex pair is an order of magnitude larger than the vacancy energy.

### A. Properties of vacancies in a pinned vortex lattice

In 1993, Ao and Thouless [11] proved that the existence of a Magnus force is a universal essence of a superconductor vortex line. In 1998, Ao [4] further established a set of processes leading to the Hall effect as a result of moving vacancies in a background of pinned vortex lattice(s). This theory manifests, in particular, that neither a modification of the vortex equation nor an assumption of two types of carriers is necessary. One only needs to study the vortex dynamics equation proposed by Niu, Ao, and Thouless [31] in 1994. To recite the theory, we turn to a crucial quantitative result regarding the motion of vacancies in a pinned vortex lattice used in the subsequent analysis, namely, the vacancy formation energy in a flux-line lattice.

First, we look at the energy scale of dislocations in the lattice. In a type-II superconductor with mixed states, the many-body correlation between the vortices and the pinning forces usually cannot be ignored. On a two-dimensional flux-line lattice (FLL) of a thin film of thickness  $d$ , spontaneous nucleation of a pair of edge dislocations costs an energy [26,32]

$$e_d(r) \cong da^2 \left( \frac{c_{66}}{4\pi} \right) \ln \left( \frac{r}{a} \right), \quad (7)$$

where  $a = (2\Phi_0/\sqrt{3}B)$  is the lattice spacing,  $r \gg a$  is the distance between two dislocations, and  $c_{66}$  is the shear modulus of the FLL; cf. Ref. [33]. For uniform distortions the elastic moduli [32] of a triangular FLL reads

$$c_{66} \approx \left( \frac{B\Phi_0}{16\pi\lambda^2\mu_0} \right) \left( 1 - \frac{1}{2\kappa^2} \right) (1 - b^2)(1 - 0.58b + 0.29b^2). \quad (8)$$

Here,  $\lambda^2 = (m^*c^2/8\pi\rho_s e^2)$  is the London penetration depth (with the effective mass  $m^*$  and superfluid density  $\rho_s$  of the underlying carriers of charge  $2e$ ),  $\Phi_0 = (hc/2|e|)$  is the flux quantum of a Cooper pair,  $\kappa$  is the Ginzburg-Landau (GL) parameter, and  $b = H/H_{c2}$  (with the applied magnetic field strength  $H$  and the upper critical field  $H_{c2}$  of the superconductor). The 2D FLL is then a uniaxial elastic medium similar to that of an isotropic and bulk superconductor. In the limit of large  $\kappa$  and relatively small magnetic field, we have

$$c_{66} \approx \left( \frac{B\Phi_0}{16\pi\lambda^2\mu_0} \right). \quad (9)$$

Using Eqs. (7)–(9), we can reexpress the energy for a dislocation pair as

$$e_d(r) = \frac{d\varepsilon_0}{2\sqrt{3}\pi} \ln\left(\frac{r}{a}\right). \quad (10)$$

Here, the major variable  $\varepsilon_0 \equiv (\Phi_0/4\pi\lambda)^2$  defines the vortex creation energy per unit length;  $(d\varepsilon_0)$  then sets the scale for both the vortex-vortex and strong pinning interactions [4]. The energy scale  $(\varepsilon_0/2\sqrt{3}\pi)$  for the dislocation pair is about ten times smaller than  $\varepsilon_0$ ; it is energetically favorable to have close-distance dislocation pairs in the lattice as carriers of transverse current.

Thus at temperature  $k_B T \ll (d\varepsilon_0)$  we can ignore the contribution to the current from the vortices hopping out of pinning as well as thermal activation of vortex-antivortex pairs. This is because the entire vortex lattice, formed via intervortex interactions should be effectively pinned down. Instead, we should look into the vacancies and interstitials which can be viewed as the smallest dislocation pairs [34]. The vacancy formation energy  $\varepsilon_v$  per unit length can be estimated [4] by setting  $r \sim 2a$  in  $e_d(r)$  together with an extra factor

$$\varepsilon_v \sim \frac{\varepsilon_0 \ln 2}{2\sqrt{3}\pi} \left( \frac{a}{\xi} \right). \quad (11)$$

Note that in Ao's initial valuations [4], the effect of the magnetic field on the energy barrier in the activation process has been ignored. It is anticipated that such an effect should relate to the ratio of the lattice constant as a function of a magnetic field to the coherence length  $\xi$  in some way. In this paper, we attempt to take the effect into account with the simplest multiplication factor  $(a/\xi)$ .

### B. Vacancy activation energy under a magnetic field

We can now analyze the experimental data from the SM of Ref. [21] with the Arrhenius empirical formula, whose validity in solid-state kinetics has been illustrated in, e.g., Ref. [35]. Taking that the dominant source of resistance  $R$  is the thermal activation of the dissipative vacancies in the

superconductor film, we have

$$R = A \exp(E_a/k_B T) \Rightarrow \log_{10} R(T) = \log_{10} A - (\log_{10} e)[E_a(T)/k_B T], \quad (12)$$

where  $A$  is a prefactor for the exponential term and  $T$  is the temperature with  $k_B$  being the usual Boltzmann constant. Both  $A$  and the activation energy  $E_a$  can be themselves temperature dependent. Now in the GL analysis, the penetration depth  $\lambda(T)$  is given by

$$\lambda(T) = \lambda(0)/[1 - (T/T_c)]^{1/2}. \quad (13)$$

The length scale is greatly affected by temperature, while its dependence on the magnetic field is negligible [36]. Substituting  $\lambda(T)$  into the vacancy formation energy equation (11), we get

$$E_a(T) = \frac{d \ln 2}{2\sqrt{3}\pi} \left( \frac{a}{\xi} \right) \left( \frac{\Phi_0}{4\pi\lambda(T)} \right)^2. \quad (14)$$

Observe that the fitting requires the magnetic field  $B$  to be in the middle of the lower critical magnetic field  $H_{c1}$  and the upper critical magnetic field  $H_{c2}$ . Although for thicker films the thickness in Eq. (12) depends on various parameters such as magnetic field, pinning, temperature, and anisotropy, the case here is relatively simple. We take  $d$  to be 50% of the *physical* thickness of the thin film, which is based on the observation that the ratio roughly corresponds to the ‘‘superconductive’’ portion of the material (along the  $c$  axis).

To proceed further, we set  $\lambda(0) = 2690 \text{ \AA}$  [37] for BSCCO-2212, which can be compared with other values from (i) reversible magnetization,  $\lambda \approx 2100 \text{ \AA}$  [38]; (ii) muon spin rotation ( $\mu$ SR),  $\lambda \approx 1800 \text{ \AA}$  [39]; and (iii) lower critical field measurements,  $\lambda \approx 2700 \text{ \AA}$  [40]. The superconducting transition temperature  $T_c = 89 \text{ K}$  and  $\log_{10} A \approx 2$  are read off from the experimental figure [21] for the BSCCO-2212 film. Other experimental parameters include the effective film thickness = 50% of a three-layer film  $d = 1.5$  unit cells (UC) =  $2 \times 1.5 \times 15.35 \times 10^{-8} \text{ cm}$  (the half height of a unit cell in Bi-2212 is  $15.35 \text{ \AA}$  [41]), the GL parameter  $\kappa = 86$  [42], and the coherence length  $\xi = \lambda(T)/\kappa$ , together with the flux quantum of the Cooper pair  $\Phi_0 = hc/2|e| = 2.07 \times 10^{-7} \text{ G cm}^2$  and the Boltzmann constant  $k_B = 1.38 \times 10^{-16} \text{ erg/K}$ . All quantities are in cgs units. We then apply Eq. (12) to Fig. 7 of the SM in Ref. [21]. The result that requires no extra fitting parameter is shown in Fig. 3. The theoretical values of the average energy of vacancy formation under diverse magnetic fields are presented in Table I. Both display excellent agreement between theory and experiment, with no adjustable parameters.

### C. Vortex-antivortex pairs in the absence of a magnetic field

In the zero-field case, the activation  $E_a(T)$  is of the order of an independent vortex energy  $\varepsilon_{\text{in}}$ , which reads [26]

$$\varepsilon_{\text{in}} = d \left( \frac{\Phi_0}{4\pi\lambda(T)} \right)^2 \ln \kappa. \quad (15)$$

For a vortex-antivortex pair, the distant current contribution cancels out; hence the item  $\ln \kappa$  should drop out. Therefore, for an impact pair, the creation energy can be taken as

$$E_a(T) = 2d \varepsilon_{\text{in}}. \quad (16)$$

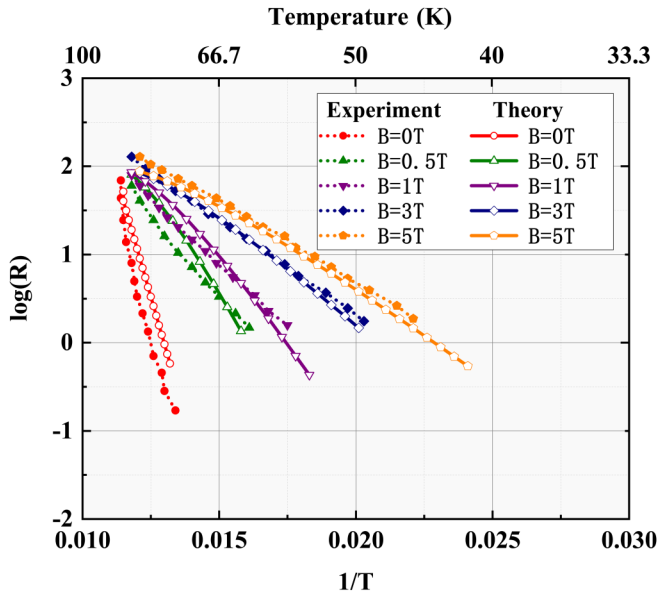


FIG. 3. An Arrhenius plot of the resistance vs temperature with the solid symbols and dotted lines from the experimental data [21] and the open symbols and solid lines from Eq. (12). The solid lines show the results when there is an external magnetic field and the activation energy is governed by the vacancy motion, which is determined by Eq. (14). In the absence of an external magnetic field, the activation energy is caused by the independent vortex motion, which depends on Eq. (16).

Substituting the above formula along with parameters taken for the other estimates into Eq. (12), we can compare the result with Fig. 7 of the SM in Ref. [21]. The outcome with no further variables again is shown in Fig. 3, with the calculated average formation energy of the vortex-antivortex pair in Table I. Both the field-dependent and zero-field predictions are in excellent agreement with experimental measurements. They are further discussed below.

#### D. A comparison of vacancy and vortex-pair activation energies

Equation (12) states that the slopes of the curves in Fig. 7 of the SM in Ref. [21] match  $E_a/k_B$ . Their average values are tabulated in Table I. Observe that the activation energy at zero field,  $B = 0$ , is an order of magnitude larger than that at  $B > 0$ , which represents one of the primary outcomes of this paper. For  $B = 0$  there are no vacancies, and the activation energy

TABLE I. The energy of the 3-UC BSCCO film with various magnetic fields. The experimental value is the activation energy of the film, which is calculated with Eq. (12). The theoretical values of the film at  $B = 0$  T and  $B \neq 0$  T are determined by Eqs. (16) and (14), respectively.

	$B$ (T)				
	0	0.5	1	3	5
Experimental $E_a$ value (K)	1273	368.3	293.0	218.5	188.7
Theoretical $E_a$ value (K)	2414	412.5	330.8	205.6	172.9

is of the same order of magnitude as the independent vortex energy.

On the other hand, the prime contribution to the activation energy comes from vacancies for  $B \neq 0$ , and the influence of the independent vortex is very small and can be ignored beyond the likely melting temperature  $T_m$ ; cf. Fig. 2. Keeping the same temperature, the films under a magnetic field have much larger resistance than they have under a zero field; cf. Fig. 7 of the SM in Ref. [21]. The corresponding activation energies at  $B \neq 0$  T are all of the same order of magnitude as the vacancy formation energies in Table I.

By quantitative comparisons between their experimental and theoretical values, we conclude that the Hall anomaly is a consequence of many-body vortex interactions, which further conforms to the theoretical analysis of the vacancy model. In particular, according to the above analysis and Table I, the vortex-antivortex energy is an order of magnitude larger than the vacancy energy. The latter constitutes one of our primary arguments.

#### IV. DISCUSSION

The current microscopic understandings of the Hall anomaly in the three-unit-cell (3-UC) BSCCO crystal may be classified into two opposite physical models, which are based on disparate theoretical approaches and give contradictory interpretations. Ao [4] fabricated BSCCO that was a few unit cells thick and detected the reversal depicted by vortex dynamics in this system. This laid the foundation to differentiate diverse models experimentally. Zhao *et al.* [21] have made a theoretical explanation based on the individual vortex dynamic model. Inversely, Ao proposed a multibody correlation model [4] in which vacancy movements on a pinned vortex lattice are the primary mechanism for the phenomenon.

In this paper we elaborate, via quantitative analysis, on the three main aspects of Ao's model [4]. Firstly, the precondition and theoretical basis of the Hall anomaly warrant the vacancy model in a pinned vortex lattice or fragments of the lattice. Secondly, both theory and experiment reveal that the energy of the vortex-antivortex pair is about an order of magnitude higher than the vacancy energy. Last but not least, distinct theoretical models of the Hall anomaly can be quantitatively distinguished via experiment. Particularly, our theoretical predictions have no adjustable parameters. As discussed in Sec. C of the SM [16], several predictions of the vacancy model explain the Hall anomaly of BSCCO in the mixed state better than some other models [14,43–47].

Note that the vacancy model is only applicable to 2D materials, requiring the thickness of the film to be limited to a few lattice lengths. This is due to, as seen in Eqs. (14) and (16), the fact that the activation energy is proportional to the thickness. Moreover, the superconducting cuprate layers interact between them via weak Josephson coupling [48,49]. With an increase in the film thickness, the layered structure causes two novel phenomena, pancake vortices and Josephson strings; that is, twisting will take place and changes the effective thickness. Both render the model useless. Experimental extraction of monolayers from bulk material, however, turns out to be extremely challenging. Though bulk high-temperature superconductors are stable under ambient conditions, thinned monolayers are highly prone to chemical degradation [50,51].

We also look forward to providing a macro-theoretical framework for related topics in future works. For example, Yang *et al.* [52] observed linear-in-temperature and linear-in-magnetic-field resistance on nanopatterned  $\text{YBa}_2\text{Cu}_3\text{O}_{7-\delta}$  (YBCO) film arrays over extended temperature and magnetic field ranges. Meanwhile, the low-field magnetoresistance oscillates with a period dictated by the superconducting flux quantum. It is possible that the unexpected signatures may be explained by a pinned vortex lattice model in a similar consideration. In particular, the plasticity of a vortex lattice pinned by periodic nanoholes can diminish the supercurrent

as a consequence of free-energy minimization. Further exploration will be presented elsewhere.

### ACKNOWLEDGMENTS

R.G. is grateful to Prof. Chuanbing Cai, Shanghai Key Laboratory of High Temperature Superconductors, Shanghai University, for useful discussions on the research. This work was supported in part by National Natural Science Foundation of China Grant No. 16Z103060007 (P.A.).

- [1] A. Niessen and F. Staas, *Phys. Lett.* **15**, 26 (1965).
- [2] W. Reed, E. Fawcett, and Y. Kim, *Phys. Rev. Lett.* **14**, 790 (1965).
- [3] L. Onsager, *Nuovo Cimento* **6**(Suppl. 2), 279 (1949).
- [4] P. Ao, *J. Phys.: Condens. Matter* **10**, L677 (1998).
- [5] P. Nozières and W. Vinen, *Philos. Mag.: A J. Theor. Exp. Appl. Phys.* **14**, 667 (1966).
- [6] S. J. Hagen, C. J. Lobb, R. L. Greene, M. G. Forrester, and J. H. Kang, *Phys. Rev. B* **41**, 11630 (1990).
- [7] S. J. Hagen, A. W. Smith, M. Rajeswari, J. L. Peng, Z. Y. Li, R. L. Greene, S. N. Mao, X. X. Xi, S. Bhattacharya, Q. Li, and C. J. Lobb, *Phys. Rev. B* **47**, 1064 (1993).
- [8] Z. D. Wang and C. S. Ting, *Phys. Rev. Lett.* **67**, 3618 (1991).
- [9] H. Hall and W. Vinen, *Proc. R. Soc. London, Ser. A* **238**, 215 (1956).
- [10] H. Hall and W. Vinen, *Proc. R. Soc. London, Ser. A* **238**, 204 (1956).
- [11] P. Ao and D. J. Thouless, *Phys. Rev. Lett.* **70**, 2158 (1993).
- [12] D. J. Thouless, P. Ao, and Q. Niu, *Phys. Rev. Lett.* **76**, 3758 (1996).
- [13] H. Xu, X. Zhu, and D. Yin, *Phys. Lett. A* **301**, 470 (2002)..
- [14] L. Ghenim, J.-Y. Fortin, G. Wen, X. Zhang, C. Baraduc, and J.-C. Villegier, *Phys. Rev. B* **69**, 064513 (2004).
- [15] B. Josephson, *Phys. Lett.* **16**, 242 (1965).
- [16] See Supplemental Material at <http://link.aps.org/supplemental/10.1103/PhysRevB.106.104507> for additional computational works and a comparison of the theory with experiment.
- [17] X.-M. Zhu, E. Brändström, and B. Sundqvist, *Phys. Rev. Lett.* **78**, 122 (1997).
- [18] X. M. Zhu and E. B. Nyeanchi, *Phys. Rev. B* **64**, 012508 (2001).
- [19] Y. Yu, L. Ma, P. Cai, R. Zhong, C. Ye, J. Shen, G. Gu, X. Chen, and Y. Zhang, *Nature (London)* **575**, 156 (2019).
- [20] H. Richter, W. Lang, M. Peruzzi, H. Hattmansdorfer, J. Durrell, and J. Pedarnig, *Supercond. Sci. Technol.* **34**, 035031 (2021).
- [21] S. Y. Zhao, N. Poccia, M. G. Panetta, C. Yu, J. W. Johnson, H. Yoo, R. Zhong, G. D. Gu, K. Watanabe, T. Taniguchi, S. V. Postolova, V. M. Vinokur, and P. Kim, *Phys. Rev. Lett.* **122**, 247001 (2019).
- [22] U. Gasser, C. Eisenmann, G. Maret, and P. Keim, *Chem. Phys. Chem.* **11**, 963 (2010).
- [23] J. Kosterlitz and D. Thouless, *J. Phys. C: Solid State Phys.* **6**, 1181 (1973).
- [24] D. R. Nelson and B. I. Halperin, *Phys. Rev. B* **19**, 2457 (1979).
- [25] D. R. Nelson, *Phys. Rev. B* **18**, 2318 (1978).
- [26] G. Blatter, M. Feigelman, V. Geshkenbein, A. Larkin, and V. Vinokur, *Rev. Mod. Phys.* **66**, 1125 (1994).
- [27] P. Ao, *Phys. Rev. Lett.* **124**, 249701 (2020).
- [28] P. L. Gammel, L. F. Schneemeyer, J. V. Waszczak, and D. J. Bishop, *Phys. Rev. Lett.* **61**, 1666 (1988).
- [29] H. Safar, P. L. Gammel, D. A. Huse, D. J. Bishop, W. C. Lee, J. Giapintzakis, and D. M. Ginsberg, *Phys. Rev. Lett.* **70**, 3800 (1993).
- [30] P. L. Gammel, A. F. Hebard, and D. J. Bishop, *Phys. Rev. Lett.* **60**, 144 (1988).
- [31] Q. Niu, P. Ao, and D. J. Thouless, *Phys. Rev. Lett.* **72**, 1706 (1994).
- [32] E. Brandt, *Rep. Prog. Phys.* **58**, 1465 (1995).
- [33] J. Kosterlitz, *Rep. Prog. Phys.* **79**, 026001 (2016).
- [34] J. Friedel, *Dislocations*, International Series of Monographs on Solid State Physics Vol. 3 (Elsevier, New York, 2013).
- [35] B. Mossel, B. Bhandari, B. D'Arcy, and N. Caffin, *LWT-Food Sci. Technol.* **33**, 545 (2000).
- [36] A. Pippard, *Proc. R. Soc. London, Ser. A* **203**, 210 (1950).
- [37] R. Prozorov, R. Giannetta, A. Carrington, P. Fournier, R. Greene, P. Guptasarma, D. Hinks, and A. Banks, *Appl. Phys. Lett.* **77**, 4202 (2000).
- [38] V. G. Kogan, M. Ledvij, A. Y. Simonov, J. Cho, and D. C. Johnston, *Phys. Rev. Lett.* **70**, 1870 (1993).
- [39] S.L. Lee, P. Zimmermann, H. Keller, M. Warden, I. M. Savic, R. Schauwecker, D. Zech, R. Cubitt, E. M. Forgan, P. H. Kes, T.W. Li, A. A. Menovsky, and Z. Tarnawski, *Phys. Rev. Lett.* **71**, 3862 (1993).
- [40] M. Nideröst, R. Frassanito, M. Saalfrank, A. C. Mota, G. Blatter, V. N. Zavaritsky, T. W. Li, and P. Kes, *Phys. Rev. Lett.* **81**, 3231 (1998).
- [41] Z. Dou, Y. Lu, C. Song, X. Ma, and Q. Xue, *Sci. Sin. Phys. Mech. Astron.* **48**, 087404 (2018).
- [42] S. Stintzing and W. Zwerger, *Phys. Rev. B* **56**, 9004 (1997).
- [43] S. Y. Zhao, N. Poccia, M. G. Panetta, C. Yu, J. W. Johnson, H. Yoo, R. Zhong, G. D. Gu, K. Watanabe, T. Taniguchi, S. V. Postolova, V. M. Vinokur, and P. Kim, *Phys. Rev. Lett.* **124**, 249702 (2020).
- [44] G. Zechner, W. Lang, M. Dosmailov, M. A. Bodea, and J. D. Pedarnig, *Phys. Rev. B* **98**, 104508 (2018).
- [45] W. Göb, W. Liebich, W. Lang, I. Puica, R. Sobolewski, R. Rössler, J. Pedarnig, and D. Bäuerle, *Phys. Rev. B* **62**, 9780 (2000).
- [46] Y. Mawatari, *Phys. Rev. B* **59**, 12033 (1999).
- [47] N. Nakai, N. Hayashi, and M. Machida, *Phys. Rev. B* **83**, 024507 (2011).

- [48] L. Bulaevskii, *Int. J. Mod. Phys. B* **04**, 1849 (1990).
- [49] S. Artemenko and Y. I. Latyshev, *Mod. Phys. Lett. B* **06**, 367 (1992).
- [50] L. Sandilands, A. Reijnders, A. Su, V. Baydina, Z. Xu, A. Yang, G. Gu, T. Pedersen, F. Borondics, and K. S. Burch, *Phys. Rev. B* **90**, 081402 (2014).
- [51] K. S. Novoselov, D. Jiang, F. Schedin, T. Booth, V. Khotkevich, S. Morozov, and A. K. Geim, *Proc. Natl. Acad. Sci. USA* **102**, 10451 (2005).
- [52] C. Yang, H. Liu, Y. Liu, J. Wang, D. Qiu, S. Wang, Y. Wang, Q. He, X. Li, P. Li, Y. Tang, J. Wang, X. C. Xie, J. M. Valles Jr, J. Xiong, and Y. Li, *Nature (London)* **601**, 205 (2022).